

SiliconPV: March 25-27, 2013, Hamelin, Germany

## A comparison of models to optimize Partial Rear Contact solar cells

Andres Cuevas<sup>a\*</sup>, Di Yan<sup>a</sup>, Felix Haase<sup>b</sup>, Jan H. Petermann<sup>b</sup>, Rolf Brendel<sup>b,c</sup>

<sup>a</sup>Research School of Engineering, The Australian National University, Canberra, ACT 0200, Australia

<sup>b</sup>Institute for Solar Energy Research Hameln (ISFH), 31860 Emmerthal, Germany

<sup>c</sup>Institute for Solid State Physics, Leibniz University of Hanover, 30167 Hanover, Germany

---

### Abstract

The optimization of solar cells with localized rear contacts usually requires numerical simulation. Here we compare Sentaurus Device to a simpler Conductive Boundary (CoBo) simulator and to an approximate Geometric model. Optimization examples are given for devices with linear rear contacts in low and high injection conditions. The three modelling tools are in good agreement for high quality devices with negligible bulk and rear surface recombination. Discrepancies between the three models, generally small, are identified and explained.

© 2013 The Authors. Published by Elsevier Ltd. Open access under [CC BY-NC-ND license](https://creativecommons.org/licenses/by-nc-nd/4.0/).

Selection and/or peer-review under responsibility of the scientific committee of the SiliconPV 2013 conference

*Keywords:* modelling; Partial Rear Contact solar cells

---

### 1. Introduction

The design of advanced industrial silicon solar cells with localised rear contacts in the form of lines together with a well passivated rear surface is of high interest both for laboratories and industry. Here we compare three different computer simulation tools, Sentaurus Device [1], the Conductive Boundary (CoBo) approach proposed by Brendel [2], and an approximate geometric model proposed by Cuevas [3]. They have different degrees of complexity and accessibility. The first entails considerable training and, as we show here, careful attention to setting up the device parameters. The CoBo model simplifies the simulation by treating dopant profiles as conductive boundaries (CoBo). The boundaries are characterized by a recombination current pre-factor and a sheet resistance. This enables the direct implementation of measured values for those parameters in the simulation. The CoBo model is significantly faster than

---

\* Corresponding author. Tel.: +612 6125 3702; fax: +612 6125 0506.

E-mail address: [Andres.cuevas@anu.edu.au](mailto:Andres.cuevas@anu.edu.au).

Sentaurus Device since it requires much fewer mesh points due the avoidance of dopant profiles. The geometric model is the simplest of the three, but its accuracy and range of applicability are more restricted. To test the models, we have performed simulations in low- and high-injection conditions. Establishing the surface boundary conditions in high injection is not a trivial matter, particularly in Sentaurus Device, and can lead to significant discrepancies. Nevertheless, once these conditions have been properly established we find good agreement between the three models.

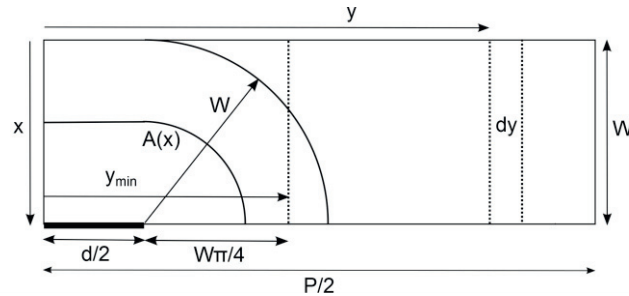


Fig. 1. Cross-sectional diagram of a half unit PRC solar cell. Drawn to scale for a contact dimension  $d=200\ \mu\text{m}$ , wafer thickness  $W=180\ \mu\text{m}$  and pitch  $p=550\ \mu\text{m}$ .  $y_{min}$  designates the boundary between the near-contact region and the lateral region.

## 2. Brief description of the geometric model

Let us consider Partial Rear Contact (PRC) solar cells having linear contacts of width  $d$  separated a distance (or pitch)  $P$ . An  $n^+$  electron transport layer is formed on a  $p$ -type silicon wafer, whose rear surface is passivated by a dielectric except where the localized metal contacts are formed. A localized  $p^+$  hole transport layer is sometimes implemented underneath the contacts to reduce recombination and contact resistance. It is sufficient to restrict the calculations to a half unit solar cell containing just one rear contact and having a rectangular aperture area  $A_0=P/2 \times 1\text{cm}$  defined by the pitch  $P$  and a unit length of 1 cm. The metal contact fraction therefore is  $f_c=d/P$ .

In a simplified geometric approach, we can divide the PRC cell into a near-contact region and a peripheral, or lateral region, as depicted in Fig. 1. The boundary between both, labelled  $y_{min}$  in Fig. 1, is related to the extent that the contact exerts its high recombination influence, which we assume equal to the wafer thickness. From geometrical considerations in Fig. 1, discussed in detail in [3],  $y_{min}=d/2+W\pi/4$ . Electrons generated in the periphery flow laterally via the  $n^+$  front diffusion, which offers a low resistance path. Within the near-contact region some electrons flow vertically down towards the rear contact to recombine there. They do so by crowding within a diminishing cross-sectional area [4],

$$A(x) = 1\text{cm} [d + \pi(W - x)]/2 \quad (1)$$

The consequences of this shrinking area can be described by means of position-dependent *effective* diffusion coefficient,

$$D_{n(\text{crowding})}(x) = D_n \frac{A(x)}{A_0} = D_n \frac{d + \pi(W - x)}{P} \quad (2)$$

Similarly, holes generated in the periphery flow laterally via the *p-type* base region, losing some energy as they do so in the form of an electrochemical potential drop in that direction, which may be interpreted as a series resistance effect. Once they reach the near-contact region holes crowd within a shrinking cross-sectional area, also given by (1), as they flow towards the hole-collecting localized contact. This results in a second electrochemical potential drop, that is, an additional series resistance effect.

The geometric model can be implemented in a 1D+1D numeric solution of the semiconductor equations by replacing the electron and hole diffusivities by their effective values [4]. A key simplification is to assume that at a given position  $y$  in the lateral region the excess carrier density is vertically uniform. This is appropriate in many cases of practical interest for high performance silicon PRC solar cells, where the minority carrier diffusion length is greater than the wafer thickness and the rear surface is well passivated.

### 3. Boundary conditions at the surfaces of the solar cell

When solving the continuity equation for minority carriers, the boundary conditions that the carrier density profile must satisfy come from the fact that the rate at which carriers flow towards a given surface must be equal to the rate at which they recombine there. If the surface recombination velocity at the contact  $S_{cont}$  is known, the excess carrier concentration at the back contact,  $n_b$ , can be related to the flux of electrons that reach that surface located at  $x=W$ ,

$$\frac{J_n(W)}{q} = n_b S_{cont} \quad (3)$$

where  $J_n(W)$  is the electron current at that position and  $q$  is the elementary charge. When applying this expression to the 1D+1D geometric model, we need to multiply  $S_{cont}$  by the fraction of the near-contact region occupied by the contact, that is, by  $d/2y_{min}$  (see Fig. 1). Commonly, surface recombination is characterised by means of an effective surface recombination velocity. Although this parameter is in general a function of the carrier injection level and of the specific parameters that characterise the surface defects, it is frequently assumed that low injection conditions apply and that  $S_{cont}$  takes a constant value.

The use of a constant surface recombination velocity in high-injection conditions can, however, be problematic. An alternative representation of surface recombination, particularly appropriate when a  $p^+$  diffused region is present, is by means of a recombination current pre-factor  $J_{0cont}$ ,

$$J_n(W) = J_{0cont} \frac{(p_0 + n_b) n_b}{n_i^2} \quad (4)$$

where  $p_0$  is the equilibrium hole concentration,  $n_b$  is the excess electron concentration at the back and  $n_i$  is the intrinsic carrier concentration. In the analysis of the near-contact region in the Geometric model we need to multiply  $J_{0cont}$  by  $d/2y_{min}$ . The two alternative representations of surface recombination are not always equivalent. To understand this, let us re-write (4) for the case of a *p-type* semiconductor where  $p_0$  is approximately equal to the acceptor density  $N_A$ ,

$$J_n(W) = J_{0cont} \frac{n_b N_A}{n_i^2} + J_{0cont} \frac{n_b^2}{n_i^2} \quad (5)$$

In low injection, the second term of (5) can be neglected, and it is possible to establish an equivalency between  $S_{cont}$  and  $J_{0cont}$ ,

$$S_{cont(lowinj)} = J_{0cont} \frac{N_A}{qn_i^2} \quad (6)$$

This equivalency is only valid in low injection conditions. In moderate and high injection conditions the second term of (5) cannot be neglected. If the boundary condition (3) is used instead of (4), surface recombination will be underestimated. This means that, to study arbitrary injection cases, the surface boundary conditions should *not* be expressed in terms of a constant surface recombination velocity. This point will be illustrated below, when applying Sentaurus Device to a high-injection case.

Both the geometric model and CoBo establish the surface boundary conditions by means of recombination current pre-factors,  $J_0$ . Recombination losses at the front  $n^+$  diffusion are proportional to the electron hole product at the front, and to the corresponding  $J_{0f}$ ,

$$R_{front} = J_{0f} \frac{(p_0 + n_f)n_f}{qn_i^2} \quad (7)$$

where  $n_f$  is the electron concentration at the front end of the base region. In the areas where it is passivated, recombination at the rear surface can be evaluated via (4) using the appropriate  $J_{0(pass)}$  or, if preferred, by an injection dependent surface recombination velocity  $S_{pass}$ , if the relevant fundamental recombination parameters of the passivated interface are known.

## 4. Comparison between models

### 4.1. Simulation parameters

As a representative example of a partial rear contact cell structure, we study the case of  $d=100 \mu\text{m}$  wide line rear contacts and vary the separation between them  $P$  to find its optimum value. Recombination at the front surface is characterized in both the geometric model and in CoBo by means of a recombination current pre-factor  $J_{0f}=10^{-13} \text{A}\cdot\text{cm}^{-2}$ . The diffused region is idealised as a conductive sheet with a sheet resistance of  $35 \Omega$ . It also produces a lateral voltage drop due to the flow of electrons through it, but this contribution is much smaller than that due to holes flowing across the base region.

Seeking a close equivalent to that boundary condition, we have implemented in Sentaurus a front  $n^+$  diffused region having a Gaussian dopant profile with a surface concentration of  $10^{20} \text{cm}^{-3}$  and a junction depth of  $1 \mu\text{m}$  (defined at a base doping of  $1 \times 10^{16} \text{cm}^{-3}$ ), together with a front surface recombination velocity of  $1.5 \times 10^4 \text{cm}\cdot\text{s}^{-1}$ . Such diffused region presents a sheet resistance of  $26 \Omega$ , and a recombination pre-factor  $J_{0f}=1.16 \times 10^{-13} \text{A}\cdot\text{cm}^{-2}$ . These values are only slightly different from those used in CoBo and in the geometric model, and lead to a possible discrepancy of about 2 mV in  $V_{oc}$ .

CoBo and the geometric model use  $n_i = 9.696 \times 10^9 \text{cm}^{-3}$  at 300 K. Sentaurus uses a slightly different value of  $n_i$ , as a consequence of including band gap narrowing effects, even in the base region of the solar cell. This results in  $n_{i(eff)} = 1.14 \times 10^{10} \text{cm}^{-3}$  for a base doping of  $1 \times 10^{16} \text{cm}^{-3}$ . The different values of  $n_i$  can lead to discrepancies of about 4 mV in  $V_{oc}$ .

The photogeneration corresponds to that produced by the AM1.5G spectrum, together with front surface texturing and a good back surface mirror. There is a small difference in the total photogenerated current between the three models. In the metal-contacted areas of a real PRC solar cell the

photogeneration is slightly lower, due to a lower back reflectivity, but given that they occupy only a small fraction of the device, neglecting this difference does not produce large errors. The calculations do not include shading or resistive losses due to a front metal grid, nor any contact resistance between metal and semiconductor. In the results presented below we have only included intrinsic (Auger and band to band) bulk recombination and set to zero the recombination at the passivated areas of the rear surface.

#### 4.2. Comparison between the models for 1D solar cells with a full area rear contact

To assess the impact of possible differences in the material parameters and in the photogeneration rate, we start by comparing solar cells with a full area rear contact where the problem is one dimensional. Tables 1 and 2 show the results for wafer dopant densities of  $N_A=10^{16} \text{ cm}^{-3}$  and  $N_A=10^{15} \text{ cm}^{-3}$  and two different rear surface recombination conditions. The latter have been chosen so that they are equivalent for both wafer dopant densities. Although the agreement between the three models is good, there are some differences. For example, for the  $N_A=10^{16} \text{ cm}^{-3}$  base doping,  $V_{oc}(Geom)$  is 4 mV higher than  $V_{oc}(Sent)$  when the rear surface recombination velocity is high. On the other hand, when the rear surface is passivated,  $V_{oc}(Sent)$  is nearly 5 mV higher than  $V_{oc}(Geom)$ . Although small, these discrepancies should be clarified by further work. Within this study, they indicate that the reliability of the simulations should be deemed to be within 5 mV in terms of  $V_{oc}$  and  $0.5 \text{ mA/cm}^2$  in terms of  $J_{sc}$ .

Table 1. Electrical parameters for 1D solar cells with full rear contacts as determined by the three simulation programs. Dopant density  $N_A=10^{16} \text{ cm}^{-3}$ , wafer thickness  $W=180 \text{ }\mu\text{m}$ .

$N_A=10^{16} \text{ cm}^{-3}$	Sentaurus	CoBo	Geometric	Sentaurus	CoBo	Geometric
	$S_{cont}=1 \times 10^6 \text{ cm/s}$ , $J_{0cont}=1.5 \text{ nA/cm}^2$			$S_{cont}=1 \times 10^3 \text{ cm/s}$ , $J_{0cont}=1.5 \text{ pA/cm}^2$		
$V_{oc}$ (mV)	600.2	601.4	604.5	634.3	628.7	629.6
$J_{sc}$ (mA/cm <sup>2</sup> )	35.93	36.54	36.05	38.81	38.81	38.63
FF	0.8272	0.8285	0.8281	0.8341	0.8334	0.833

Table 2. Electrical parameters for 1D solar cells with full rear contacts as determined by the three simulation programs. Dopant density  $N_A=10^{15} \text{ cm}^{-3}$ , wafer thickness  $W=180 \text{ }\mu\text{m}$ . Note that although the values of  $J_{0cont}$  are the same as in Table 1, in high injection it is not appropriate to describe contact recombination by means of  $S_{cont}$ .

$N_A=10^{15} \text{ cm}^{-3}$	Sentaurus	CoBo	Geometric	Sentaurus	CoBo	Geometric
	$J_{0cont}=1.5 \text{ nA/cm}^2$			$J_{0cont}=1.5 \text{ pA/cm}^2$		
$V_{oc}$ (mV)	539.6	539.8	539.5	621	618.7	621
$J_{sc}$ (mA/cm <sup>2</sup> )	36.75	36.91	36.45	39.98	39.98	40.05
FF	0.810	0.8164	0.811	0.829	0.8307	0.829

#### 4.3. PRC solar cell, low injection example

Figs. 2 and 3 show the simulation results for  $N_A=10^{16} \text{ cm}^{-3}$  and  $S_{cont}=10^6 \text{ cm}\cdot\text{s}^{-1}$  surface recombination velocity, representative of the kinetic limit for carrier velocity. This is characterized in the geometric and CoBo models by means of recombination current pre-factor  $J_{0cont}=1.5 \times 10^{-9} \text{ A}\cdot\text{cm}^{-2}$ . A second set of

simulation results for  $S_{cont}=10^3 \text{ cm} \cdot \text{s}^{-1}$ , that is,  $J_{0cont}=1.5 \times 10^{-12} \text{ A} \cdot \text{cm}^{-2}$ , is also presented. Globally, a good agreement between the three simulators is observed.

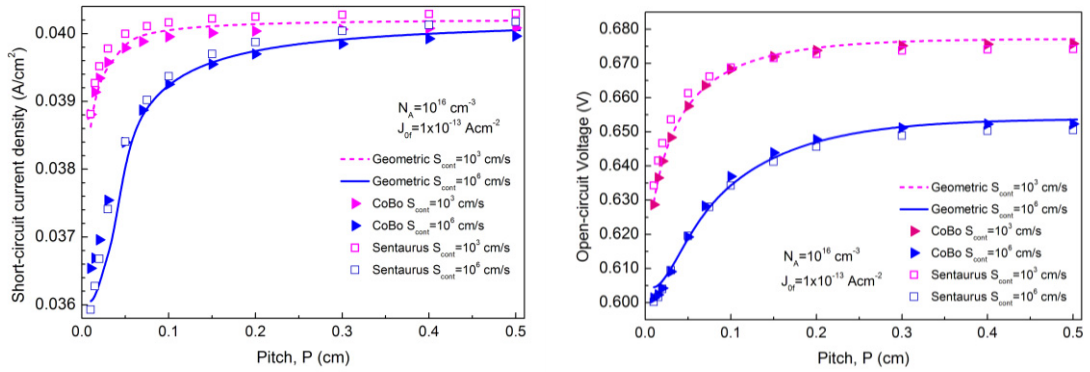


Fig. 2. Short-circuit current density and open-circuit voltage as a function of the pitch for  $N_A=10^{16} \text{ cm}^{-3}$ ,  $d=100 \mu\text{m}$ ,  $W=180 \mu\text{m}$ ,  $J_{0f}=10^{-13} \text{ Acm}^{-2}$ . Two cases of contact recombination are shown, characterized by  $J_{0cont}=1.5 \times 10^{-12} \text{ Acm}^{-2}$  or  $J_{0cont}=1.5 \times 10^{-9} \text{ Acm}^{-2}$  (Geometric and CoBo models) and by  $S_{cont}=10^3 \text{ cm} \cdot \text{s}^{-1}$  or  $S_{cont}=10^6 \text{ cm} \cdot \text{s}^{-1}$  (Sentaurus).

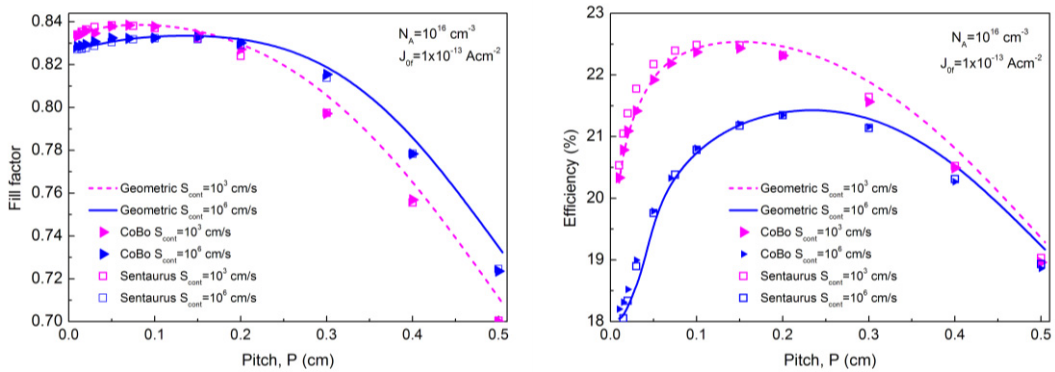


Fig. 3. Fill factor and efficiency as a function of the pitch for  $N_A=10^{16} \text{ cm}^{-3}$ ,  $d=100 \mu\text{m}$ ,  $W=180 \mu\text{m}$  and  $J_{0f}=10^{-13} \text{ Acm}^{-2}$ . Two cases of contact recombination are shown, characterized by  $J_{0cont}=1.5 \times 10^{-12} \text{ Acm}^{-2}$  or  $J_{0cont}=1.5 \times 10^{-9} \text{ Acm}^{-2}$  (Geometric and CoBo models) and by  $S_{cont}=10^3 \text{ cm} \cdot \text{s}^{-1}$  or  $S_{cont}=10^6 \text{ cm} \cdot \text{s}^{-1}$  (Sentaurus).

The short-circuit current density,  $J_{sc}$ , increases with the pitch. This trend is particularly significant for the high contact recombination case, as shown in Fig. 2. Sentaurus gives slightly higher  $J_{sc}$  values than the other two models for high pitch values, probably as a result of an interpolation of the photogeneration as a function of position.

As it may be expected,  $V_{oc}$  increases as the fraction of metal-contacted area is reduced. The reason is that carriers generated in the peripheral region that surrounds the rear contact are injected into the near-contact region, where they contribute to increase the carrier concentration and hence the local voltage, that is,  $V_{oc}$ . Interestingly,  $V_{oc}$  saturates at a lower value when the surface recombination velocity at the

contact is high. This is because for large pitch values (large peripheral area), many carriers recombine in-situ, and they do not contribute to boosting the carrier population in the near-contact region; beyond a certain pitch, no more carriers are transferred laterally and  $V_{oc}$  no longer increases. As mentioned above, and as Fig. 2 indicates, the disagreement between the models in terms of  $V_{oc}$  is usually less than 5 mV.

The fill-factor degrades quite strongly with the distance that carriers have to travel laterally. The agreement in FF between Sentaurus and CoBo is excellent, whereas the geometric model gives slightly optimistic values. The conversion efficiency, also shown in Fig. 3, presents a maximum of 21.4% for a pitch of 0.2 cm for a high contact recombination, or a maximum of 22.5% at a pitch of 0.15 cm for the case of a well passivated contact.

#### 4.4. PRC solar cell, high injection example

In a second example, we consider a wafer doping of  $N_A=10^{15} \text{ cm}^{-3}$ , corresponding to a resistivity of  $13.5 \Omega \cdot \text{cm}$ . It only makes sense to use such high resistivity if a  $p^+$  region is created in the vicinity of the rear contact. Accordingly, we now assume a low contact recombination, characterized by means of  $J_{0cont}=1.5 \times 10^{-12} \text{ A} \cdot \text{cm}^{-2}$ . If low injection conditions applied, the surface recombination velocity corresponding to  $N_A=10^{15} \text{ cm}^{-3}$  would be  $S_{cont}=10^2 \text{ cm} \cdot \text{s}^{-1}$ . Using this constant value of  $S_{cont}$  as a boundary condition in Sentaurus leads to an over-estimation of  $V_{oc}$ , as shown in Fig. 4. In reality, for this lowly doped wafer with well passivated contacts, high carrier injection conditions do occur, and using a constant  $S_{cont}$  as a boundary condition is inadequate, since it leads to an underestimation of recombination losses. Therefore, we have also performed Sentaurus simulations with a boundary condition of  $J_{0cont}=1.5 \times 10^{-12} \text{ A} \cdot \text{cm}^{-2}$ . To implement this boundary condition in Sentaurus, we created a  $p^+$  region having a Gaussian dopant profile with a surface concentration of  $5 \times 10^{18} \text{ cm}^{-3}$ , a junction depth of  $1 \mu\text{m}$  and a surface recombination velocity of  $1.15 \times 10^5 \text{ cm} \cdot \text{s}^{-1}$ . As Fig. 4 indicates, the resulting  $V_{oc}$  is now in good agreement with the other two models.

The short-circuit current density  $J_{sc}$  drops rapidly for pitch values larger than 0.4 cm. This unexpected trend is confirmed by the three models. Convergence problems made it impossible to obtain a result for  $P=0.5\text{cm}$  with Sentaurus, but CoBo and the geometric model are in excellent agreement. The reason for this behavior is that for  $P>0.4$  cm practically all the carriers generated far from the contact recombine in-situ, mostly at the front  $n^+$  region. That is, the distant peripheral regions effectively operate in open-circuit and do not contribute to the terminal current. If the short-circuit current was plotted, then it would tend towards an asymptotic value. The decrease of the short-circuit current density  $J_{sc}$  results from dividing the total, nearly constant current by an increasing device area. It can also be observed that Sentaurus predicts a higher  $J_{sc}$  than the other two models in the intermediate pitch range. This is probably due to differences in the photogeneration rate as a function of depth in the silicon wafer. Sentaurus performs an interpolation of the generation data points that can result in small discrepancies, such as those in Fig. 4. For this high resistivity wafer, the conversion efficiency, shown in in Fig. 5, presents a maximum of about 22% for a pitch of 0.075 cm, both values slightly lower than those corresponding to the  $1.5 \Omega \cdot \text{cm}$  wafer.

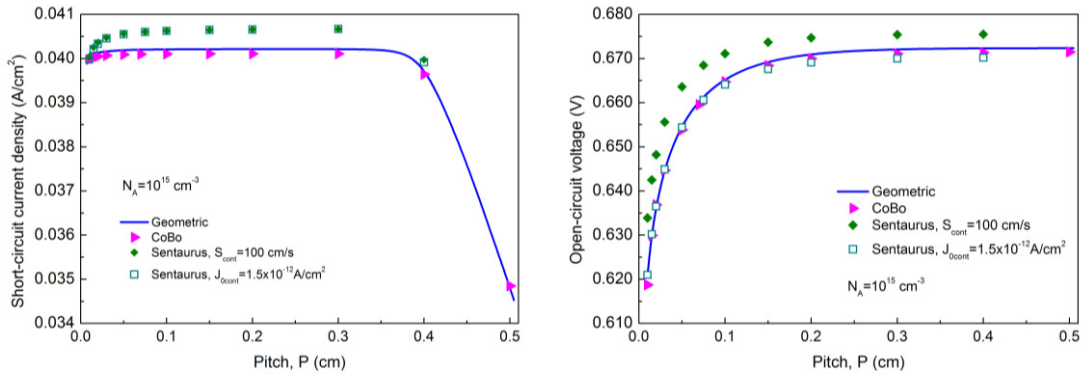


Fig. 4. Short-circuit current density and open-circuit voltage as a function of the pitch for  $N_A=10^{15} \text{ cm}^{-3}$ ,  $d=100 \text{ }\mu\text{m}$ ,  $W=180 \text{ }\mu\text{m}$ ,  $J_{0f}=10^{-13} \text{ Acm}^{-2}$ . Contact recombination is characterized by  $J_{0cont}=1.5 \times 10^{-12} \text{ Acm}^{-2}$  (Geometric and CoBo models) and either by  $S_{cont}=10^2 \text{ cm}\cdot\text{s}^{-1}$  or  $J_{0cont}=1.5 \times 10^{-12} \text{ Acm}^{-2}$  (Sentauros).

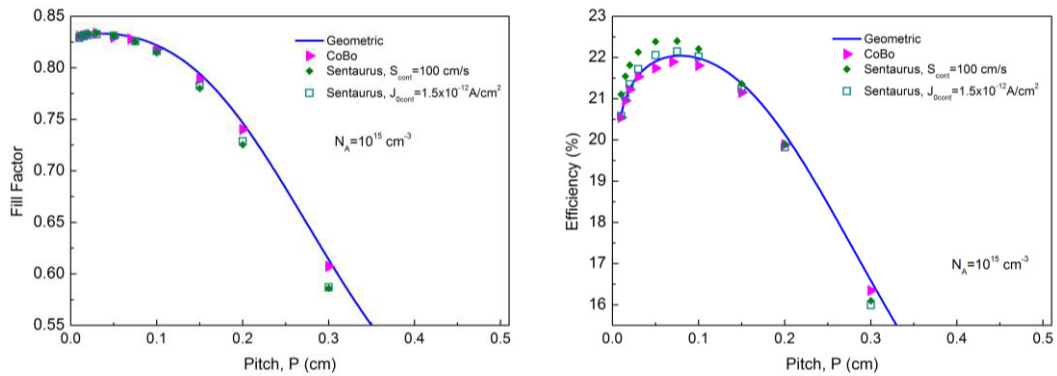


Fig. 5. Fill factor and efficiency as a function of the pitch for  $N_A=10^{15} \text{ cm}^{-3}$ ,  $d=100 \text{ }\mu\text{m}$ ,  $W=180 \text{ }\mu\text{m}$  and  $J_{0f}=10^{-13} \text{ Acm}^{-2}$ . Contact recombination is characterized by  $J_{0cont}=1.5 \times 10^{-12} \text{ Acm}^{-2}$  (Geometric and CoBo models) and either by  $S_{cont}=10^2 \text{ cm}\cdot\text{s}^{-1}$  or  $J_{0cont}=1.5 \times 10^{-12} \text{ Acm}^{-2}$  (Sentauros).

## 5. Conclusions

The boundary conditions implemented in solar cell simulations can have a significant influence on the analysis of devices in high injection conditions. This paper has shown that establishing the boundary conditions in terms of recombination current pre-factors  $J_0$  is more robust. With these boundary conditions, the agreement between CoBo and Sentauros Device is excellent both in low and high injection cases. In cases where the only significant recombination occurs at the front  $n^+$  diffusion or at the rear metal contact, the Geometric model is also in good agreement with the other two simulation tools, even in the challenging case of high injection. Nevertheless, if significant bulk or surface recombination takes place, the use of CoBo or Sentauros Device is recommended. Neither CoBo, nor the Geometric model, include the details of generation-recombination mechanisms in the highly doped  $n^+$  and  $p^+$  regions of the

solar cell. They do not include either the details of space charge regions. Sentaurus Device offers full modeling capabilities, but these are not essential to study the main traits of PRC solar cell operation.

The iterative implementation of the geometric model may be regarded as a numerical analysis, just like the other two. Significant differences of complexity do, however, exist between the three simulation tools. The geometric model has been implemented in Microsoft Excel, with 100 cells in the peripheral region and 200 in the near-contact region. The number of cells has not been optimized, but it is likely that it could be reduced. In comparison, CoBo and Sentaurus use a matrix of up to 4500 mesh points, depending on the size of the unit cell. Needless to say, they can be expected to be more accurate and, above all, more general. It is worth noting, however, that computational accuracy can be secondary to the selection of appropriate parameters for the physical properties of silicon. The simpler CoBo and Geometric modeling tools are, in that regard, more versatile. The Geometric model offers a good balance between physical insight and accuracy, even if it is restricted to high lifetime, well-passivated silicon wafers.

## References

- [1] Sentaurus Process User Guide, Version E-2010-12, 2010.
- [2] Brendel, R. Modeling solar cells with the dopant-diffused layers treated as conductive boundaries. *Progress in Photovoltaics: Research and Applications* 2012; **20**(1): 31-43.
- [3] Cuevas, A. Geometrical Analysis of Solar Cells With Partial Rear Contacts. *IEEE Journal of Photovoltaics*, 2012. **2**(4): 485-493.
- [4] Cuevas, A. Physical model of back line-contact front-junction solar cells. *Journal of Applied Physics* 2013; **113**: 164502.